OFFPRINT

Variable enstrophy flux and energy spectrum in two-dimensional turbulence with Ekman friction

MAHENDRA K. VERMA

Please visit the new website
www.epljournal.org

Variable enstrophy flux and energy spectrum in two-dimensional turbulence with Ekman friction

MAHENDRA K. VERMA[(a)]

Department of Physics, Indian Institute of Technology - Kanpur, 208016 India

Abstract – Experiments and numerical simulations reveal that in the forward cascade regime, the energy spectrum of two-dimensional turbulence with Ekman friction deviates from Kraichnan's prediction of k^{-3} power spectrum. In this letter we explain this observation using an analytic model based on variable enstrophy flux arising due to Ekman friction. We derive an expression for the enstrophy flux which exhibits a logarithmic dependence in the inertial range for the Ekman-friction–dominated flows. The energy spectrum obtained using this enstrophy flux shows a power law scaling for large Reynolds number and small Ekman friction, but has an exponential behaviour for large Ekman friction and relatively small Reynolds number.

Physics of turbulent flow is quite complex. One of the important and generic features of turbulent flow in three dimensions (3D) is a constant energy flux from large length scales to small length scales. The wave numbers exhibiting constant energy flux have $k^{-5/3}$ energy spectrum [1]. Two-dimensional (2D) fluid turbulence, however, has significantly different behavior. Kraichnan [2] showed that in 2D turbulence, the low wave number modes (below the forcing wave number) exhibit inverse energy cascade, while the large wave number modes have forward enstrophy (square of the vertical vorticity) cascade. These two regimes have $k^{-5/3}$ and k^{-3} energy spectra, respectively. The above features have been observed in numerical simulations [3–6], and in experiments involving electromagnetically driven flows [7,8] and soap films [9,10]. The atmospheric data indicates that some features of the atmospheric turbulence are two-dimensional [11,12].

The fluid flow in a two-dimensional surface is also affected by the drag from its environment as demonstrated by several experiments [13–17] and numerical simulations [18,19]. This kind of friction is also referred to as "Ekman friction". Belmonte *et al.* [13] performed experiments on freely suspended soap films, and reported that the energy spectrum is steeper than k^{-3}. Boffetta *et al.* [17] observed a similar steepening of the spectrum in their experiment on a thin layer of ionic fluids, which is driven electromagnetically and is moving under a layer of fresh water. Here, the drag on the ionic fluid is induced by the shear layer induced by fresh water [14,17]. Nam *et al.* [18] and Boffetta *et al.* [19] performed numerical simulations with Ekman friction and reported the spectral exponent to be larger than 3.

The aforementioned steepening of the energy spectrum in two-dimensional flow has been attributed to Ekman friction, which is modeled as $-\alpha\mathbf{u}$, where α is a constant, and $\mathbf{u}$ is the velocity field. Nam *et al.* [18] and Boffetta *et al.* [17] attempted to derive the new spectral indices using an analogy with the dynamics of a scalar in a turbulent fluid. They postulated that a fluid blob has a finite lifetime $\tau = \alpha^{-1}$, and it is passively advected. The turbulent motion leads to a stretch of a fluid blob with a mean rate given by the Lyapunov exponent λ. Using the above assumption, the incompressibility condition, and the mean-field approximation, Boffetta *et al.* [17] predicted that the energy spectrum $E(k) \sim k^{-3-2\alpha/\lambda}$. Boffetta *et al.* [19] also studied the intermittency effects of Ekman friction, and showed that the small-scale statistics of the vorticity fluctuations is related to the passive scalar transported by the velocity field. Perleker and Pandit [20] performed detailed numerical simulation and studied the effects of Ekman friction on the structure function. They showed that the velocity structure functions display simple scaling. The reader is also referred to a review article by Kellay and Goldburg [16].

(a)E-mail: mkv@iitk.ac.in

The arguments of Boffetta *et al.* [17] involves several assumptions and relatively complex computation of the Lyapunov exponent. In the present letter we compute the energy spectrum using a model based on a variable enstrophy flux. Unlike the viscous force, which affects the dissipation range, Ekman friction is active at all scales. As a result, the enstrophy flux decreases significantly in the inertial range itself. This decrease in the flux leads to a steepening of the energy and enstrophy spectra. In the present letter, we will derive an expression for the variable enstrophy flux in terms of the dissipative parameters α, the kinematic viscosity ν, and other turbulence parameters. We will show that the variable enstrophy flux yields an energy spectrum steeper than k^{-3}.

The dynamical equations for the vertical vorticity in a two-dimensional fluid flow with Ekman friction are

$$\frac{\partial \omega}{\partial t} + \mathbf{u}\cdot\nabla\omega = -\alpha\omega + \nu\nabla^2\omega + f(t), \qquad (1)$$

and the incompressibility constraint $\nabla\cdot\mathbf{u} = 0$, which implies that the density of the fluid is a constant. In the above equation, $\mathbf{u}$ is the velocity field, $\omega = (\nabla\times\mathbf{u})_z$ is the vertical component of the vorticity field, and ν is the kinematic viscosity of the fluid. An external force $f(t)$ is applied to maintain a steady state.

The enstrophy flux $\Pi(k)$ is defined as the total enstrophy transferred from the modes inside the wave number sphere of radius k to the modes outside the sphere. Since the above flux is defined in the wave number space, we rewrite eq. (1) in the Fourier space as

$$\frac{\partial \omega(\mathbf{k})}{\partial t} = -ik_j \sum_{\mathbf{q}} u_j(\mathbf{q})\omega(\mathbf{k}-\mathbf{q}) - \alpha\omega(\mathbf{k}) - \nu k^2\omega(\mathbf{k}) + f(\mathbf{k}),$$
$$(2)$$

where $\mathbf{k}$ is the wave number. The corresponding enstrophy evolution equation is

$$\frac{\partial Z(k)}{\partial t} = T(k) - 2\alpha Z(k) - 2\nu k^2 Z(k) + F(k), \qquad (3)$$

where $Z(k) = |\omega(\mathbf{k})|^2/2$ is the one-dimensional enstrophy spectrum, $T(k)$ is the enstrophy transfer term arising due to nonlinearity, and $F(k)$ is the enstrophy supply rate due to the forcing [1]. It has been analytically shown that the total energy $E = \sum |\mathbf{u}(\mathbf{k})|^2/2$ and the total enstrophy $Z = \sum |\omega(\mathbf{k})|^2/2$ are conserved in the inviscid limit ($\nu = 0$ and $\alpha = 0$) without any external forcing [1,2]. The dual energy spectrum described in the introduction is a consequence of simultaneous conservation of energy and enstrophy [2]. Two-dimensional turbulent flow with $\alpha = 0$ and $\nu \to 0$ exhibits $k^{-5/3}$ energy spectrum for $k < k_f$, and k^{-3} energy spectrum for $k > k_f$, where k_f is the center of the forcing wave number band. The scenario changes significantly when $\alpha \neq 0$, as observed in earlier experiments and numerical simulations.

The forcing wave number in a typical experiment on Ekman friction is of the order of the box size. Consequently, experiments report only forward enstrophy cascade and energy spectrum as k^{-a} with $a \geqslant 3$. Since $|\omega(k)| = k|\mathbf{u}(k)|$, the enstrophy spectrum would vary as k^{-a+2}. Pope [1] prescribed a function for the energy spectrum for three-dimensional fluid turbulence. We adapt Pope's function for the enstrophy spectrum $Z(k)$ as

$$Z(k) = C(\Pi(k))^{2/3}k^{-1}f_L(kL)f_\eta(k\eta), \qquad (4)$$

where $C \approx 1.4$ is a constant (equivalent to Kolmogorov's constant for 3D fluid turbulence) [21,22], $\Pi(k)$ is the enstrophy flux emanating from the wave number sphere of radius k, and $f_L(kL)$, $f_\eta(k\eta)$ specify the components of the forcing scale and dissipative-scale enstrophy spectra, respectively. These functions have been described by Pope [1] as

$$f_L(kL) = \left(\frac{kL}{[(kL)^2 + c_L]^{1/2}}\right)^{1+p_0}, \qquad (5)$$

$$f_\eta(k\eta) = \exp\left[-\beta\left\{[(k\eta)^4 + c_\eta^4]^{1/4} - c_\eta\right\}\right], \qquad (6)$$

where L is the box size, and c_L, c_η, p_0, β are constants, which are determined by matching the function of eq. (4) with experimental observations. In the absence of any clear prescription for these constants, we take $C_L \approx 6.78$, $c_\eta \approx 0.40$, $\beta \approx 5.2$ and $p_0 = 2$, used by Pope [1] for 3D turbulence.

In Kraichnan's phenomenology for the two-dimensional fluid turbulence without Ekman friction, the enstrophy flux $\Pi(k)$ is a constant in the inertial range. This is due to the fact that in this regime, the local dissipation rate ($2\nu k^2 Z(k)$) is negligible, and the forcing is absent. However, in the presence of Ekman friction, $\Pi(k)$ decreases in the inertial range itself due to the $2\alpha Z(k)$ term. The enstrophy fluxes $\Pi(k+dk)$ differs from $\Pi(k)$ by the rate of enstrophy loss in the wave number shell $(k, k+dk)$, *i.e.*,

$$\Pi(k+dk) - \Pi(k) = -\left\{2\nu k^2 + 2\alpha\right\}Z(k)dk, \qquad (7)$$

or

$$\frac{d\Pi(k)}{dk} = -\left\{2\nu k^2 + 2\alpha\right\}C(\Pi(k))^{2/3}k^{-1}f_\eta(k\eta). \qquad (8)$$

In the present letter, we focus on the inertial and dissipative ranges. Therefore, we have ignored the variation of the forcing scale spectrum $f_L(kL)$, *i.e.*, $f_L(kL) \approx 1$.

Equation (8) can be easily integrated, which yields

$$\left[\frac{\Pi(k)}{\Pi_0}\right]^{1/3} = 1 - \frac{2C}{3}\frac{\nu}{\Pi_0^{1/3}\eta^2}I_1(k\eta) - \frac{2\alpha C}{3\Pi_0^{1/3}}I_2(k\eta)$$
$$= 1 - \frac{2C}{3}C_1 I_1(k\eta) - \frac{2\alpha C}{3\Pi_0^{1/3}}I_2(k\eta), \qquad (9)$$

where Π_0 is the maximum value of the enstrophy flux at $k = k_1$ (which is also the lower limit for the integration), $C_1 = \nu/(\Pi_0^{1/3}\eta^2)$ is a constant, and

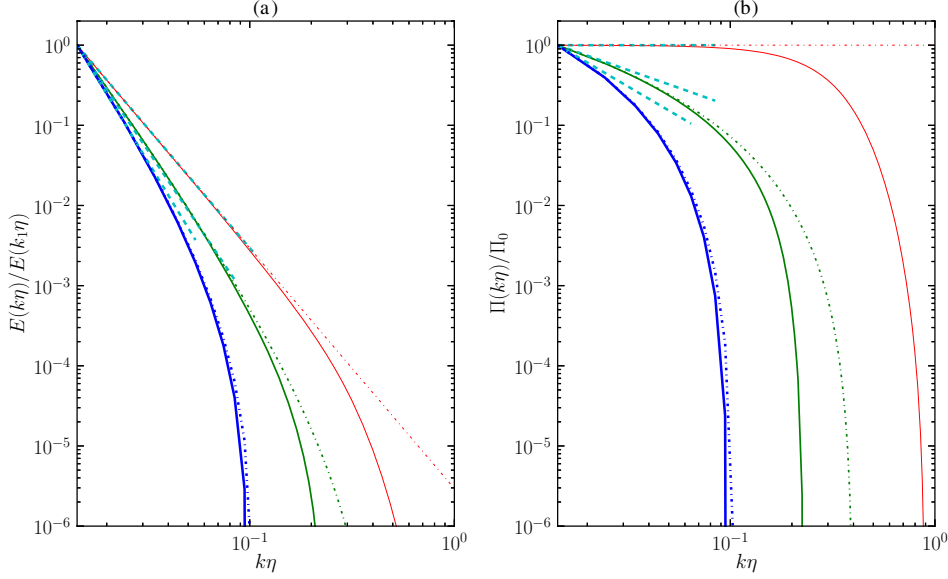$$\eta = \frac{1}{\sqrt{C_1}}\frac{\sqrt{\nu}}{\Pi_0^{1/6}} \qquad (10)$$

Fig. 1: (Colour on-line) (a) Plots of energy spectra for $Re = 10^6$ and $\alpha' = 0$ (red thin curve), 0.3 (green curve), and 0.5 (blue thick curve). The best-fit curves k^{-a} with $a = 3, 3.8$ and 4.2 are plotted as dashed cyan lines. The approximate energy spectrum using the approximate enstrophy flux of eq. (13) is exhibited as chained lines. (b) Plots of the corresponding enstrophy flux (solid lines), the approximate enstrophy flux of eq. (13) (chained lines), and its power law approximation described by eq. (14) (cyan dashed lines).

is the Kolmogorov length for two-dimensional turbulence. For all our calculations, we also take the constant C to be 1.4 [21,22]. The integrals I_1 and I_2 are

$$I_1(k\eta) = \int_{k_1\eta}^{k\eta} \mathrm{d}k' k' f_\eta(k'), \qquad (11)$$

$$I_2(k\eta) = \int_{k_1\eta}^{k\eta} \mathrm{d}k' k'^{-1} f_\eta(k'), \qquad (12)$$

where the lower limit for the wave number k_1 is chosen to be $6 \times 2\pi/L$ [1]. Pope [1] suggests that the inertial range starts around this wave number. Using eq. (10) and $\Pi_0 = U^3/L^3$, we can deduce that $k_1\eta = 6(2\pi/L)\eta = 12\pi/\sqrt{C_1 Re}$. In our model the enstrophy flux peaks at $k = k_1$ and decreases for higher values of k. Equation (9) shows that the enstrophy flux depends critically on the nondimensional parameter $\alpha' = 2\alpha C/(3\Pi_0^{1/3})$.

The form of eq. (9) appears quite complex, but it can be easily approximated in the inertial range in the $\nu \to 0$ limit. Under this limit, $I_1(k) \approx 0$ and $I_2(k) \approx \alpha' \log(k/k_1)$. Therefore, the approximate enstrophy flux would be

$$\frac{\Pi(k)}{\Pi_0} \approx [1 - \alpha' \log(k/k_1)]^3, \qquad (13)$$

which shows that for nonzero α', the enstrophy flux decreases logarithmically with the increase of wave number. We will show later that for turbulent flows, the above approximate function matches quite well with that computed using eq. (9) in the inertial range.

Additionally, the wave numbers satisfying the condition $\alpha' \log(k/k_1) \ll 1$ follow a power law behavior:

$$\frac{\Pi(k)}{\Pi_0} \approx e^{-3\alpha' \log(k/k_1)} \approx (k/k_1)^{-3\alpha'}. \qquad (14)$$

Once we have computed the k-dependent enstrophy flux, the enstrophy spectrum can be immediately derived as

$$Z(k) = \begin{cases} C\Pi_0^{2/3} k^{-1} f_\eta(k\eta) \left[\frac{\Pi(k)}{\Pi_0}\right]^{2/3}, & \text{if } k > k_1, \\ C\Pi_0^{2/3} k^{-1} f_L(kL), & \text{otherwise,} \end{cases} \qquad (15)$$

while the energy spectrum varies as

$$E(k) = \begin{cases} C\Pi_0^{2/3} k^{-3} f_\eta(k\eta) \left[\frac{\Pi(k)}{\Pi_0}\right]^{2/3}, & \text{if } k > k_1, \\ C\Pi_0^{2/3} k^{-3} f_L(kL), & \text{otherwise.} \end{cases} \qquad (16)$$

For a narrow range of the inertial range with $\alpha' \log(k/k_1) \ll 1$, the aforementioned equations yield

$$E(k) \sim C\Pi_0^{2/3} k^{-3-2\alpha'}. \qquad (17)$$

We can also compute the enstrophy dissipation rates due to the viscous force and Ekman friction using $D_\nu(k) = \int_0^\infty 2\nu k^2 Z(k)\mathrm{d}k$ and $D_\alpha(k) = \int_0^\infty 2\alpha Z(k)\mathrm{d}k$, respectively. Another important quantity is the ratio of the nonlinear term and Ekman friction, which can be estimated using $Re_\alpha = U/(\alpha L)$, termed as "Reynolds number based on Ekman friction". We will show later that Re_α plays an important role in determining the structure of the energy spectrum.

We use the aforementioned model to study the nature of energy spectrum as a function of the Ekman friction

Table 1: Table depicting our model calculation for the Reynolds number $Re = 10^6$ and $\alpha' = 0, 0.3, 0.5$ (first three rows), and for the experimental parameters of Boffetta *et al.*'s [17] (next three rows). Here α is the coefficient of the Ekman friction, u_{rms} is the rms velocity, ω_{rms} is the rms vorticity, Π_0 is the maximum value of enstrophy flux, $\alpha' = 2\alpha C/(3\Pi_0^{1/3})$ with $C = 1.4$, $Re_\alpha = U/(\alpha L)$ is the ratio of the nonlinear term and the Ekman friction term, a, a_B are the spectral exponents computed using our model and by Boffetta *et al.*, respectively, b is the coefficient of $E(k) = \exp(-b(k\eta - k_1\eta))$, and D_α/D_ν is the ratio of the dissipation rates by Ekman friction and the viscous force. For Boffetta *et al.*'s experimental parameters [17], we use $Re_\alpha = u_{rms}/(\alpha L)$ with $L = 50$ cm, and $\Pi_0 = \omega_{rms}^3$.

α (s^{-1})	u_{rms} (cm/s)	ω_{rms} (s^{-1})	Π_0 (s^{-3})	α' $-$	Re $-$	Re_α $-$	a $-$	a_B $-$	b $-$	D_α/D_ν $-$
–	–	–	–	0	10^6	∞	3	–	–	0
–	–	–	–	0.3	10^6	≈ 3	3.8	–	–	22
–	–	–	–	0.5	10^6	≈ 2	4.2	–	–	100
0.037	1.32	0.75	0.42	0.046	6600	0.71	–	3.5	16.7	0.091
0.059	1.33	0.64	0.26	0.086	6650	0.45	–	3.8	18.1	0.18
0.069	0.79	0.60	0.21	0.107	3950	0.22	–	4.0	16.8	0.16

parameter α. We take two cases: large Reynolds number, and relatively small Reynolds number. For the former case, we take $Re = 10^6$ and $\alpha' = 0, 0.3$, and 0.5, and compute the normalized enstrophy flux $\Pi(k\eta)/\Pi_0$ and energy spectrum $E(k\eta)/E(k_1\eta)$ using eqs. (9) and (16), respectively. These functions are exhibited in fig. 1 using thin red ($\alpha' = 0$), green ($\alpha' = 0.3$), and thick blue ($\alpha' = 0.5$) curves. For $\alpha' = 0$, the inertial range enstrophy flux is nearly constant and $E(k) \sim k^{-3}$, consistent with Kraichnan's predictions, more so a validation of our model. Note however that $\Pi(k)$ must vanish for wave numbers $k \gg \eta^{-1}$. We use this condition to determine the constant C_1 of eq. (9), which yields $C_1 = 7.17$.

With the increase of α' or Ekman friction, the entropy flux becomes k-dependent and the energy spectrum is steeper than k^{-3}. For $\alpha' = 0.3$ and 0.5, the spectral indices are 3.8 and 4.2, respectively. The best-fit curves are shown in fig. 1(a) using the dashed cyan lines. We also plot the approximate enstrophy flux of eq. (13) and the corresponding energy spectrum in fig. 1 as chained lines. In the inertial range, the approximate energy spectrum and the approximate enstrophy flux fit rather well with the model predictions. For a very narrow range of $k\eta$, $\Pi(k) \sim k^{-3\alpha'}$ as shown by the cyan dashed line in fig. 1(b). This result indicates that the logarithmic dependence of enstrophy flux is valid for a larger range of wave numbers than the power law of eq. (14). This observation is also consistent with the fact that the spectral index of the energy spectrum is not exactly equal to $3 + 2\alpha'$ (eq. (17)), but these two exponents are reasonably close.

We also compute Re_α for $\alpha' = 0.3$ and 0.5 and find them to be approximately 3 and 2, respectively (see table 1). This result indicates that the nonlinear term $\mathbf{u} \cdot \nabla \mathbf{u}$ dominates the Ekman friction, consistent with the power law behaviour of the energy spectrum. The ratio D_α/D_ν is 22 and 100 for $\alpha' = 0.3$ and 0.5, respectively, indicating that the Ekman friction is stronger than the viscous term. The strong wave number dependence of the enstrophy flux is due to the important role played by Ekman friction.
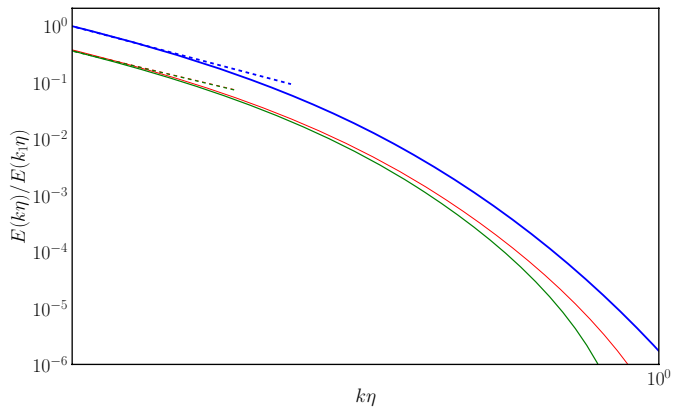

Fig. 2: (Colour on-line) Plots of the energy spectra $E^u(k\eta)/E^u(k_1\eta)$ computed using our model for the experimental parameters of Boffetta *et al.* [17] on a log-log scale. The thin red, green, and thick blue curves represent the $\alpha = 0.037, 0.059, 0.069$ experimental runs, respectively (see table 1). The power law function k^{-a} (dashed curves) does not fit with the energy spectrum.

We perform our model calculations for the experimental parameters of Boffetta *et al.* [17]. The Reynolds number for these runs ranges from 3950 to 6600, which is relatively small compared to the aforementioned test cases with $Re = 10^6$. In Boffetta *et al.*'s experiment, a thin layer of electrolyte solution of water and NaCl contained in a square tank ($L = 50$ cm) is stirred electromagnetically using four triangular shaped electromagnets with alternating signs. A layer of fresh water was kept above the electrolyte solution. The thickness of the ionic fluid was maintained at 0.3 cm, while that of the upper fluid was varied from 0.3 cm to 0.7 cm. The ionic fluid experiences a drag force $-\alpha\mathbf{u}$. The kinematic viscosity of the electrolyte is the same as that of water ($\nu \approx 0.01$ cm^2/s). For the three sets of experiments performed, Boffetta *et al.* reported the Ekman friction coefficient $\alpha = 0.037, 0.059, 0.069$, $Re = u_{rms}L/\nu = 6600, 6650, 3950$, and the spectral indices $a = 3.5, 3.8$, and 4.0, respectively. See table 1 for more details.
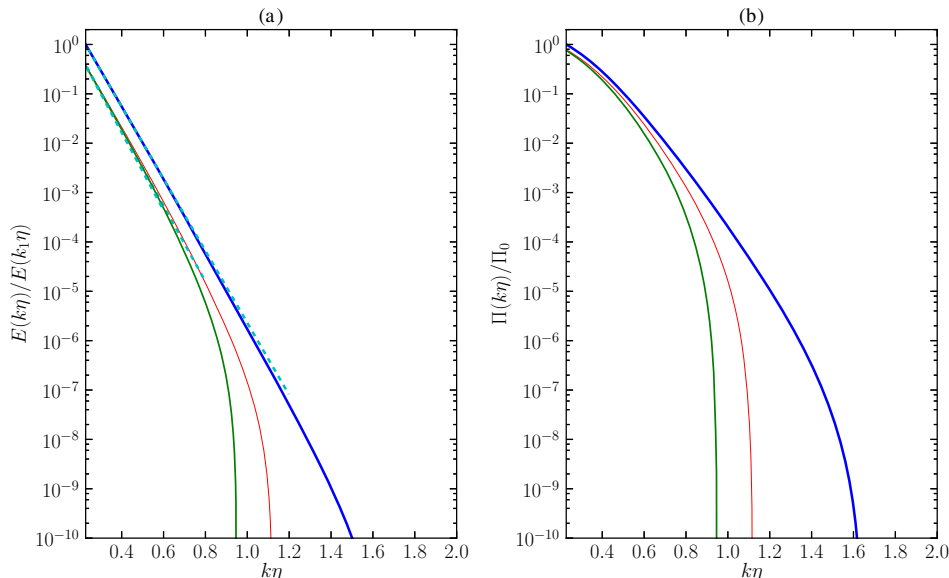
Fig. 3: (Colour on-line) (a) Plots of energy spectra for the experimental parameters of Boffetta *et al.* [17] with $\alpha' = 0.037$ (red thin curve), 0.059 (green curve), and 0.069 (blue thick curve) on a semi-log scale. See table 1 for more details. Exponential functions $\exp(-b(k\eta - k_1\eta))$ (dashed cyan lines) with $b = 16.7, 18.1$, and 16.8, respectively, are the best-fit curves for the spectra in the nonviscous range. (b) The corresponding enstrophy flux for the aforementioned experimental cases.

For the three aforementioned experimental sets of Boffetta *et al.* [17], the nondimensional parameters are $\alpha' = 0.046, 0.086, 0.107$ and $\mathrm{Re}_\alpha = U/(\alpha L) = 0.71$, $0.45, 0.22$, respectively, indicating that the nonlinear term is somewhat weaker than the Ekman friction. We also estimate the maximum enstrophy flux Π_0 as $\omega_{\mathrm{rms}}^2/T \approx \omega_{\mathrm{rms}}^3$. Using the aforementioned parameters we compute the energy spectra and the normalized enstrophy fluxes for these experimental sets using our model, and compare the results. In fig. 2 we plot the energy spectra and their best power law fits. The figure illustrates that a power law is not a good fit for the energy spectra predicted by the model. Therefore, we attempt to fit the energy spectra with an exponential function $\exp(-b(k\eta - k_1\eta))$ for $k > k_1$. In fig. 3 we plot the normalized energy spectra $E(k\eta)/E(k_1\eta)$ and normalized enstrophy flux on a semi-log scale. The exponential functions (the dashed lines) fit well with the energy spectra in the nonviscous range, and the fitting parameters b for the three experimental cases are 16.7, 18.1, and 16.8, respectively. Thus an exponential function may describe the energy spectrum of the Boffetta *et al.* better than a power law function, consistent with the observation that Ekman friction dominates the nonlinear term in these cases ($\mathrm{Re}_\alpha < 1$). Also, the approximate enstrophy flux computed using eq. (13) does not match with the model flux (eq. (9)) due to the absence of an inertial range, which is due the dominance of Ekman friction over the nonlinear term. A cautionary remark however is in order: our estimates of Π_0, Re using the experimental parameters of Boffetta *et al.*'s [17] have significant errors. Hence the model predictions are somewhat uncertain, and they need to be carefully verified using more refined experiments and numerical simulations.

In summary, we showed that Ekman friction strongly affects the enstrophy flux in two-dimensional turbulence. We derived an expression for the variable enstrophy flux in terms of Ekman friction parameter α. As a result, the kinetic energy spectrum is steeper than k^{-3}. For large Reynolds number flows with $\mathrm{Re}_\alpha = U/(\alpha L) > 1$, we expect a power law behaviour for the energy spectrum. This is due to the dominance of the nonlinear term over Ekman friction. However, Ekman friction is stronger than the nonlinear term for flows with $\mathrm{Re}_\alpha < 1$, hence an exponential energy spectrum may be expected for such flows.

The method presented here is quite general and could be applied to other situations as well. The liquid metal flows in the presence of a strong magnetic field under the quasi-static approximation [23] has a dissipation term similar to the Ekman friction. Adaption of the present procedure to the liquid metal flow would provide valuable insights into its energy spectrum and dynamics. Another important direction for future work could be the verification of our model using direct numerical simulations.

$* * *$

REFERENCES

[1] POPE S. B., *Turbulent Flows* (Cambridge University Press, Cambridge) 2000.
[2] KRAICHNAN R. H., *J. Fluid Mech.*, **47** (1971) 525.

[3] Siggia E. D. and Aref H., *Phys. Fluids*, **24** (1981) 171.

[4] Frisch U. and Sulem P. L., *Phys. Fluids*, **27** (1984) 1921.

[5] Boffetta G., *J. Fluid Mech.*, **589** (2007) 253.

[6] Tabeling P., *Phys. Rep.*, **362** (2002) 1.

[7] Sommeria J., *J. Fluid Mech.*, **170** (1986) 139.

[8] Paret J. and Tabeling P., *Phys. Rev. Lett.*, **79** (1997) 4162.

[9] Rutgers M. A., *Phys. Rev. Lett.*, **81** (1998) 2244.

[10] Vorobieff P., Rivera M. and Ecke R. E., *Phys. Fluids*, **11** (1999) 2167.

[11] Boer G. J. and Shepard T. G., *J. Atmos. Sci.*, **40** (1983) 164.

[12] Lindborg E., *J. Fluid Mech.*, **388** (1999) 259.

[13] Belmonte A., Goldburg W. I., Kellay H., Rutgers M. A., Martin B. and Wu X. L., *Phys. Fluids*, **11** (1999) 1196.

[14] Rivera M. and Wu X. L., *Phys. Rev. Lett.*, **85** (2000) 976.

[15] Rivera M., Wu X. L. and Yeung C., *Phys. Rev. Lett.*, **87** (2001) 044501.

[16] Kellay H. and Goldburg W., *Rep. Prog. Phys.*, **65** (2002) 845.

[17] Boffetta G., Cenedese A., Espa S. and Musacchio S., *Europhys. Lett.*, **71** (2005) 590.

[18] Nam K., Ott E., Antonsen T. M. and Guzdar P. N., *Phys. Rev. Lett.*, **84** (2000) 5134.

[19] Boffetta G., Celani A., Musacchio S. and Vergassola M., *Phys. Rev. E*, **66** (2002) 026304.

[20] Perlekar P. and Pandit R., *New J. Phys.*, **11** (2009) 073003.

[21] Lesieur M., *Turbulence in Fluids - Stochastic and Numerical Modelling*, 4th edition (Kluwer Academic Publishers, Dordrecht) 2008.

[22] Lindborg E. and Vallgren A., *Phys. Fluids*, **22** (2010) 091704.

[23] Knaepen B. and Moreau R., *Annu. Rev. Fluid Mech.*, **40** (2008) 25.